RESEARCH ARTICLE

Health risk prediction model of elderly patients under interpretable deep learning and nursing decision support

Xiaohuan Li, Yanjun Huang, Xiaoxiao Li, Yanhong Zhang, Yan Wang*

Medical College, Zhengzhou University of Industrial Technology, Zhengzhou, Henan 451150, China.

Received: January 29, 2026; **accepted:** June 8, 2026.

With the aggravation of an aging society, the health risk prediction and effective nursing decision-making of elderly patients have become the key issues in the medical field. The traditional prediction model lacks interpretability and is difficult to meet the needs of clinical practice. This study constructed a health risk prediction model for elderly patients based on interpretable deep learning (DL) to provide support for nursing decision-making. Massive clinical data of elderly patients were collected from multiple hospital systems. A health risk prediction model (Opti-CNN) was constructed by employing a DL algorithm and a convolutional neural network (CNN). SHapley Additive exPlanations (SHAP) and local interpretable model-agnostic explanations (LIME) were introduced to explain the model prediction results with the occurrence of hospital falls as the prediction target. The results showed that the accuracy, precision, recall, and F1-score of the constructed interpretable Opti-CNN were 86.2%, 85.8%, 86.2%, and 86%, respectively, and the area under the receiver operating characteristic (ROC) curve was 0.90, which was higher than other algorithms. LIME analysis indicated that age, coexistence of multiple diseases, psychological emotions, and multiple medications had positive effects on health risks, while nutritional supplements and listening had negative effects. SHAP value analysis clarified the contribution of each risk factor. The coexistence of multiple diseases and a debilitating state were the primary driving factors with SHAP value of 0.9. The contributions of nervous system diseases and gait balance ability were as high as 0.8, while nutritional supplements and hearing function showed negative effects. The information gain of nervous system diseases was the largest one of 0.8, and the coexistence of multiple diseases and multiple drugs was the second with both of 0.7. Based on the model's predictions and interpretable analysis, a nursing decision support system was developed to provide personalized advice. The constructed model and system offered effective tools for the health management of elderly patients, potentially enhancing healthcare quality and patient outcomes.

Keywords: interpretable deep learning; elderly patients; health risk prediction; nursing decision support.

***Corresponding author:** Yan Wang, Medical College, Zhengzhou University of Industrial Technology, Zhengzhou, Henan 451150, China. Email: 13838212169@163.com.

Introduction

With the acceleration of the global population aging process, the health management of the elderly population has become a severe challenge in the field of public health. Elderly patients are often accompanied by a variety of chronic diseases, physiological deterioration, and complex social and psychological factors, which lead to a significant increase in their health risks. The incidence of adverse events such as cardiovascular events, falls, and readmission increases, which not only seriously affects the quality of life, but also brings a heavy burden to families and social medical systems [1]. Consequently, accurate health risk prediction and early intervention for this demographic are critically important for improving prognoses, reducing medical costs, and enhancing population health.

Traditional machine learning models such as logistic regression, random forest and support vector machine (SVM) are widely utilized in health risk prediction for the elderly due to their clear principles, efficient training, and interpretability [2]. In recent years, deep learning (DL) technology has shown great potential in medical health risk prediction with its powerful features learning and nonlinear fitting capabilities [3]. DL models have made breakthroughs in processing electronic health records, medical images, and continuous monitoring data through autonomous feature extraction and complex pattern recognition [4]. Additionally, interpretable methodologies like Shapley Additive exPlanations (SHAP) and Local Interpretable Model-agnostic Explanations (LIME) have emerged as prominent tools for explaining model decisions in healthcare [5, 6]. The integration of Artificial Intelligence (AI) technologies including machine learning and DL has significantly enhanced nursing decision support systems, enabling them to address complex clinical challenges [7]. Despite these advances, critical challenges persist. Traditional machine learning models struggle with the high dimensionality, noise, temporal dynamics, and multimodal nature of medical data, limiting their predictive accuracy and ability to uncover deep data correlations [4]. DL models, while powerful, operate as "black boxes" with opaque decision-making processes, hindering clinical trust and adoption, especially in geriatric care where evidence-based causality is paramount [8, 9]. Data quality inconsistencies, low standardization, privacy constraints, and multi-center integration difficulties further complicate research [4]. Although SHAP and LIME improve model transparency, translating their outputs into clinically actionable insights while balancing interpretability fidelity remains challenging [6]. In geriatric nursing, existing decision support systems often focus on single-disease risks, lacking comprehensive evaluation capabilities for multifaceted issues like polypharmacy, functional decline, and psychosocial factors, thus failing to deliver holistic care recommendations [10].

This study developed an accurate and interpretable health risk prediction model for elderly patients by integrating interpretable DL technology to enhance the model's representation of complex health data through innovative feature engineering and DL algorithms, while leveraging SHAP and LIME to demystify decision logic and identify key risk factors including non-traditional ones. Furthermore, a nursing decision support module that translated interpretable predictions into personalized, actionable intervention strategies for clinical nurses was proposed by employing advanced feature engineering techniques and DL algorithms to optimize predictive performance. SHAP and LIME were systematically integrated to provide global and local explanations of model decisions, revealing feature contributions and interactions. The nursing decision support module was engineered to convert these explanations into user-friendly clinical protocols, prioritizing comprehensibility and operational feasibility for healthcare providers. This research addressed the critical gap between high-performance AI models and clinically trustworthy tools in geriatric care. By fusing interpretable DL with pragmatic decision support, this study enabled early risk identification, personalized interventions, and optimized resource allocation, directly improving prognosis, reducing medical costs, and enhancing elderly patients' quality of life. The proposed framework set a precedent for transparent, human-centered AI in healthcare, promoting wider adoption of predictive technologies and catalyzing advancements in evidence-based geriatric nursing practices globally.

Materials and methods

Research object and data source

In this study, the existing anonymized data of patients' medical records between January 1, 2020 and December 31, 2025 were retrospectively analyzed, and the prediction model of elderly patients' in-hospital falls was constructed and optimized. A total of 3,612 elderly anonymized inpatients were initially screened from the hospital databases. After applying inclusion criteria of age ≥ 65 years, admission to geriatrics, orthopedics, or neurology departments, a hospital stay duration of ≥ 24 hours, and the availability of complete electronic health record (EHR) data, and exclusion criteria of having experienced a fall prior to admission, being unable to move independently, having a critical medical condition resulting in a negligible risk of falling during hospitalization, or having severely incomplete data, a total of 2,300 patients were ultimately included in the study with 1,265 (55.0%) males and 1,035 (45.0%) females, aged from 65 to 98 years with a mean ± standard deviation (SD) of 74.6 ± 8.2 years. The patients were divided into the event group (patients who experienced a fall during hospitalization), comprising 450 patients, and the control group (patients who did not experience a fall), comprising 1,850 patients. The anonymized data included the EHR, hospital information system (HIS), laboratory information system (LIS), picture archiving and communication system (PACS), and nursing record system. The variables collected covered demographic characteristics including age, gender, height, weight, BMI, marital status, education level, and medical insurance type; medical history information including main diagnosis, complications, previous fall history, and operation history; drug use information including the drugs utilized during hospitalization, especially high-risk drugs, and the drug name, dosage, frequency, and duration of drug use; laboratory examination indexes including blood routine, biochemical indexes, and coagulation function; vital signs including temperature, pulse, respiration, blood pressure, and oxygen saturation during admission and hospitalization; nursing records including activity ability, sleep status, fall risk assessment records, constraints, and the use of assistive devices; end event including fall in the hospital. In-hospital falls were defined as unexpected falls to the ground or falls from bed or chair to the ground or lower level at any place during hospitalization.

Data preprocessing and feature engineering

The original data were systematically cleaned, and the missing values were filled by missing completely at random (MCAR) and missing at random (MAR). The Z-score methodology combined with clinical rationality judgment and identification was utilized to normalize the data, and the duplicate records were eliminated to ensure the data quality. Classifying variables such as gender, marital status, disease diagnosis, and drug category were subjected to One-Hot Encoding or Label Encoding. Analysis of variance (ANOVA), correlation analysis, Least Absolute Shrinkage and Selection Operator (LASSO) regression, mutual information method, recursive feature elimination (RFE), and tree-based feature importance evaluation were utilized for preliminary feature screening from statistical and model-based perspectives to reduce redundant features and model complexity. To explore the interaction effect of features and adapt to the DL model, the idea of feature crossing was innovatively utilized for reference, and the preprocessed structured data was transformed into an image representation, that was, different feature crossing strategies were studied, and the crossed high-dimensional feature matrix was transformed into a gray scale image or a pseudo-color image as the input of a convolutional neural network (CNN). Then, advantages were extracted by employing CNN image features. The processed data set was divided into a training set, a verification set, and a test set at the ratio of 7:1:2, and stratified sampling was utilized to keep the data distribution of each set consistent and ensure the reliability and objectivity of model training, superparameter tuning, and final evaluation.

Construction of an interpretable DL health risk prediction model

As a DL model, CNN could not only use a convolution kernel (CK) to extract features, reduce connections and storage requirements, and improve efficiency, but also reuse the same CK to reduce model parameters, which was suitable for processing matrix data such as image data [11]. CNN consisted of a convolution layer, a pooling layer, and a fully connected layer. For input neuron x_i, when n signals were input to neuron j at the same time, the weight value connecting each input signal with neuron j was W_{ij}, and the internal parameter offset of neuron j was b_j. Then the whole process of neuron j from receiving the input signal to generating the output signal was expressed as below.

$$y_j = g\left[b_j + \sum_{i=1}^{I}\left(W_{ij} * X_i\right)\right] \quad (1)$$

In the convolution layer, its parameters were composed of a set of kernels. During forward propagation, each kernel performed a convolution operation on the input vector of the convolution layer and then generated the corresponding feature vector. The convolution layer Y_n was calculated as follows.

$$Y_n = \sum_{i=1}^{I} W_{n,i} * X_i + b_n \quad (2)$$

where I was the number of channels. $W_{n,i}$ was the CK. X_i was the input feature map. b_n was the offset. Y_n was processed by the ReLU nonlinear activation function $g(\cdot)$ to get the final feature map Z_n as shown below.

$$Z_n = g(Y_n) \quad (3)$$

The pool layer after the convolution layer was composed of multiple feature surfaces, which was a deep excavation and refinement of the features extracted from the convolution layer. Pool layer neurons pooled the local acceptance domain, which could reduce the computational complexity, enhance the generalization ability of the model, avoid over-fitting, and improve the prediction accuracy of the model for unknown data. The common pooling methodologies were maximum pooling and average pooling, and the maximum pooling effect was better when the linear classifier was utilized in the classification layer and was calculated as follows [12].

$$Y_{n(\mu,v)} = max_{(v-1)s+1<k<vs}\left[x_{n(\mu,v)}\right] \quad (4)$$

where S was the size of the pooled CK. $n(\mu,v)$ was the v neuron of the u channel in the n^{th} layer. For the setting of full connection layer, the number of full connection layers was determined by experiments. If only one fully connected layer was utilized, the results could be directly output, otherwise, the dropout would be added to prevent over-fitting. There were many parameters in the fully connected layer, which were easy to overfit during training, resulting in weak generalization ability. However, the stability of the model could be improved by selectively turning off some neurons. For the binary classification task of predicting the health risks of elderly patients, model training needed to quantify the prediction error through a loss function to guide optimization. The model constructed in this study selected the cross-entropy loss function to evaluate the model's performance by calculating the "distance" between the true label distribution and the model's predicted probability distribution as follows.

$$L = -[m \cdot log(p) + (1-m) \cdot log(1-p)] \quad (5)$$

where m was the true label of the sample. If an elderly patient had a fall, it was recorded as 1, otherwise as 0. p was the probability that the model predicted the patient would have a fall with the value ranging from 0 to 1. CNN was a suitable modeling choice to transform observation into a single-channel pixel picture. In the model structure design, deepening and widening the network were considered to improve the model performance. Deepening the network enhanced the fitting ability of the model to nonlinear relations, while widening the network improved the feature extraction ability by increasing the number of CKs or adopting a multi-branch network design. To effectively train the Opti - CNN model, this study compared two widely used optimization algorithms of Stochastic Gradient Descent (SGD) and Adaptive Moment Estimation (Adam). SGD updated parameters one sample at a time, which was computationally efficient but might converge slowly. Adam estimated the first - and second - order moments of the gradients to dynamically adjust the learning rate of each parameter, usually having a faster convergence speed and better adaptability. The default parameters used in this study for preliminary experiments were $\eta = 0.01$ for SGD learning rate, while $\beta_1 = 0.9$, $\beta_2 = 0.999$, $\varepsilon = 10^{-8}$, $\eta = 0.001$ as Adam's parameters. The validation set loss was used as the early - stopping criterion.

Model interpretable analysis

SHAP and LIME were utilized to analyze the interpretability of the established CNN model. The core goal of SHAP was to explain the prediction result of an observation by calculating the contribution of each feature. The SHAP value of each component of the neural network was approximated by calculating the weight. The SHAP values of all components were integrated to get the SHAP value of the whole neural network as follows.

$$y_i = y_{base} + f(x_{i1}) + f(x_{i2}) + \ldots + f(x_{ik}) \quad (6)$$

where y_i was the predicted value of the model for the sample. y_{base} was the average value of the predicted values of all samples. $f(x_{i1})$ was the contribution of the corresponding feature in the *i-th* sample to the final predicted value y_i. When $f(x_{i1})$ was greater than 0, it indicated that this feature increased the predicted value. When $f(x_{i1})$ was less than 0, it meant that this feature reduced the predicted value. LIME was a partially interpretable and model-independent methodology. In this work, a new data set was constructed by covering some pixels or blocks to generate new pictures. The CNN was utilized to predict the pictures in the new data set. A new linear regression model was then trained near the target sample. In this model, high-weight pixels would be highlighted in the picture. By observing the marked picture, the pixels that had a great influence on the prediction results of the model could be understood, and the key features could be inferred in reverse. The local proxy model could be expressed as below.

$$E(x) = arg\ min\ L(f, g, \theta x) + \Omega(g) \quad (7)$$

where x was the sample. f was the original model that needed to be explained. g was a local fitting model. θx was the proximity. $\Omega(g)$ was the complexity of the model. By measuring the closeness between the original model and the local interpretable model through the loss, it could make this loss as small as possible, given that the smaller the loss, the higher the fitting degree of the local proxy model.

Design of nursing decision support module under an interpretable model

Literature reviewing, semi-structured interviews, and questionnaires were utilized to analyze the requirements of the nursing decision support system, and its core requirements included the demand for risk early warning that the system needed to be connected with the Hospital Information System (HIS)/Laboratory Information System (LIS) to realize real-time update and automatic trigger, visually display risk-related information, and support historical trend comparison; the demand for intervention advice that emphasized individualization, generated advice according to patient risk factors, marked evidence-based evidence and supporting jumping to the original text, and distinguished the intervention responsibilities of different roles; the convenience of operation that required a simple interface, adapting to the mobile terminal, and realizing

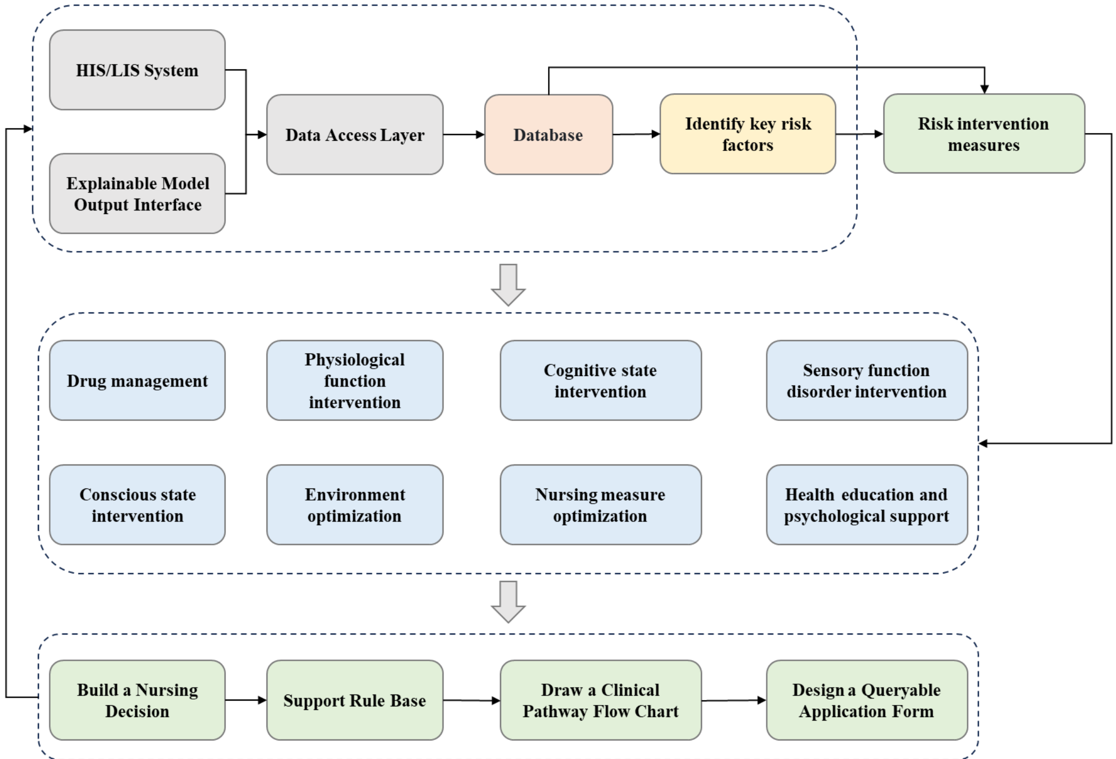

Figure 1. Nursing decision support architecture diagram.

data linkage to reduce the burden of medical operation. Based on the interpretable results, the key risk factors were identified by SHAP value and LIME local explanation. The patients were further divided into three levels according to the risk level. The individual fall risk level was generated, and the intervention risk factors were ranked to guide the allocation of nursing resources and the intervention order. Targeted and multi-level intervention strategies were then formulated, aiming at high-risk internal factors and factors that could change the external environment and care process. The intelligent nursing decision support rule base and clinical path flow chart were constructed to facilitate nurses' inquiry and adoption (Figure 1).

Model evaluation

The performance of the proposed model was evaluated on a held-out test dataset that constituted 20% of the total dataset and was randomly sampled and set aside before model development. Receiver Operating Characteristic (ROC) curve, accuracy, recall, precision, and F1-score were employed for model evaluation as shown below.

$$\text{Accuracy} = \frac{\text{TP+TN}}{\text{TP+TN+FP+FN}} \tag{8}$$

$$\text{Recall} = \frac{\text{TP}}{\text{TP+FN}} \tag{9}$$

$$\text{Precision} = \frac{\text{TP}}{\text{TP+FP}} \tag{10}$$

$$\text{F1} - \text{score} = 2 \times \frac{\text{Precision}\times\text{Recall}}{\text{Precision+Recall}} \tag{11}$$

Where TP, TN, FP, and FN were true positives, true negatives, false positives, and false negatives, respectively. ROC curve was used to assess the model's discrimination ability across various classification thresholds by plotting the true positive rate (recall) against the false positive rate (1 - specificity) at different threshold settings. The Area Under the ROC

Curve (AUC) provided a single scalar value summarizing the overall performance, where an AUC of 1.0 represented perfect discrimination, and 0.5 represented a random classifier. To comprehensively evaluate the performance of the proposed Opti-CNN model, it was compared against several representative baseline models from different algorithmic families including Multilayer Perceptron (MLP) [13], Gated Recurrent Unit (GRU) network [14], lightweight CNN architecture MobileNet [15] for the neural network models and Support Vector Machine (SVM) [16], Gradient Boosting Decision Tree (GBDT) [17], and CatBoost algorithm [18] for traditional machine learning models. All models were trained and tested on the same dataset partitions.

Test environment and platform

The programming of this study used Python 3.7.3 (https://www.python.org/), and the Deep Learning (DL) framework adopted PyTorch version 1.6.0 (https://pytorch.org/). The experimental environment was configured by employing the Anaconda distribution (https://www.anaconda.com) as the integrated platform with Jupyter Lab (https://jupyter.org/) for the presentation and analysis of experimental results. The study used Intel® Core™ i7-9750H CPU with a base frequency of 2.60 GHz, 32.00 GB of RAM, a primary 510 GB SSD, and an NVIDIA GeForce GTX 1650 graphics card under Microsoft Windows 10 Home Chinese Edition (64-bit). The initial architecture of the CNN model was configured as two convolutional layers with each containing 12 kernels of size 3 × 3 and a padding of 1, two activation layers utilizing the ReLU function, and two pooling layers, both employing max pooling over a 2 × 2 region followed by a single fully connected layer without Dropout. To systematically evaluate the impact of batch size (mini - batch size) on model performance and determine the optimal value, a special ablation experiment was designed. While keeping the initial model architecture, optimizer (Adam), learning rate (0.001), and number of training epochs (10 epochs) unchanged, a set of batch size values for the comparison experiment was selected including 10, 32, 64, 128, 200. For each set batch size, the model was independently trained and validated on the same five - fold cross - validation dataset partition. The average classification accuracy on the validation set was used as the core evaluation index to explore the relationship between the batch size and the model's generalization performance. According to the experimental results, the batch size configuration with the highest validation accuracy was selected for the construction of the final prediction model.

Results and discussion

Model parameters

The number of convolutional kernels largely determines the model's ability to extract data features. However, increasing this number does not always lead to improved model performance. Combined with the trend of pursuing simplicity in model design and the relatively small sample size of this dataset, experiments were carried out in three cases with the number of CKs as 15, 30, and 60, respectively. The results showed that the combination of CKs with the highest accuracy was 60, 60, and 30 for the first, second, and third layers, respectively (Table 1). When choosing the convolution layer size, the range was limited to 3 × 3 and 5 × 5 for comparative experiments. The results showed that varying the combination of kernel sizes across the three layers did not lead to a significant improvement in prediction accuracy. The accuracy for the eight tested combinations ranged from 85.1% to 86.1% with the configurations of (3 × 3, 3 × 3, 5 × 5), (3 × 3, 5 × 5, 3 × 3), (3 × 3, 5 × 5, 5 × 5), (5 × 5, 3 × 3, 3 × 3), (5 × 5, 3 × 3, 5 × 5), (5 × 5, 5 × 5, 3 × 3), and (5 × 5, 5 × 5, 5 × 5) achieving accuracies of 85.2%, 85.6%, 85.3%, 85.4%, 85.7%, 85.5%, and 85.1%, respectively, while the highest accuracy of 86.1% was obtained when using 3 × 3 kernels for all three layers. Therefore, the original model configuration was adopted, that was, the first, second, and third layers all used 3 × 3 convolutional kernels.

Table 1. Comparison of accuracy of different CKs.

No. of CKs in the first layer	No. of CKs in the second layer	No. of CKs in the third layer	Accuracy
15	15	15	83.20%
15	15	30	83.90%
15	15	60	83.00%
15	30	15	83.70%
15	30	30	84.40%
15	30	60	83.60%
15	60	15	83.80%
15	60	30	84.20%
15	60	60	83.50%
30	15	15	83.90%
30	15	30	84.10%
30	15	60	83.30%
30	30	15	84.30%
30	30	30	84.60%
30	30	60	84.00%
30	60	15	84.00%
30	60	30	84.50%
30	60	60	84.20%
60	15	15	84.10%
60	15	30	84.30%
60	15	60	83.80%
60	30	15	84.40%
60	30	30	84.70%
60	30	60	84.10%
60	60	15	84.50%
60	60	30	84.80%
60	60	60	84.60%

Comparative experiments were conducted with and without a batch normalization (BN) layer after the convolutional layers and with different mini-batch sizes when BN was employed. The results indicated that adding a BN layer did not improve model accuracy. Without BN and using a mini-batch size of 10, the model achieved the highest accuracy of 86.2%. When a BN layer was added with a mini-batch size of 10, the accuracy decreased to 85.8%. Further increasing the mini-batch size to 120, 220, and 320 resulted in accuracies of 85.3%, 85.6%, and 85.4%, respectively, all lower than the configuration without BN. Therefore, the BN layer was not included in the final prediction model. The comparison results of prediction model accuracy under different mini-batch values demonstrated that, with the increase of mini-batch values, the accuracy of the model generally showed an upward trend and reached the highest value when the mini-batch size was 200 (Figure 2). Therefore, the prediction model adopted the setting of mini-batch size of 200.

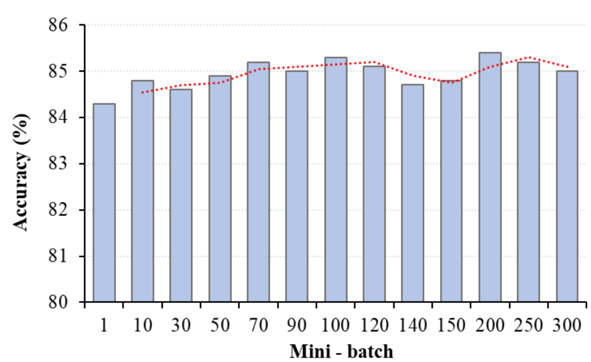

Figure 2. Comparison of accuracies for different Mini – batches.

The common choices of optimizers in CNNs were SGD and Adam. The accuracy of SGD and Adam were 84.30% and 85.20%, respectively, which showed that the Adam optimizer was better than the SGD optimizer. The influence of different epoch times on model prediction accuracy showed that, when the number of epoch times was low, the accuracy of the model gradually improved. When the number of epochs reached 10, the model accuracy reached the highest value. Since then, with the increasing number of epochs, the accuracy of the model gradually decreased (Figure 3). Therefore, 10 epochs were selected for training.

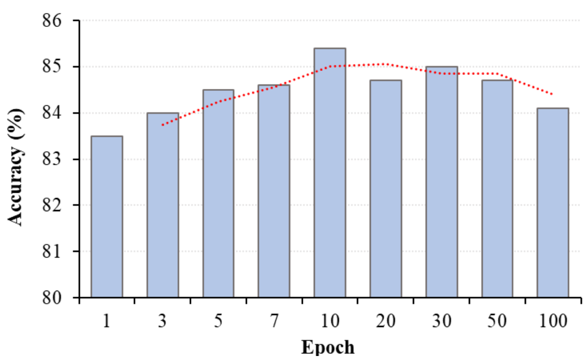

Figure 3. Comparison of accuracy rates for different numbers of epochs.

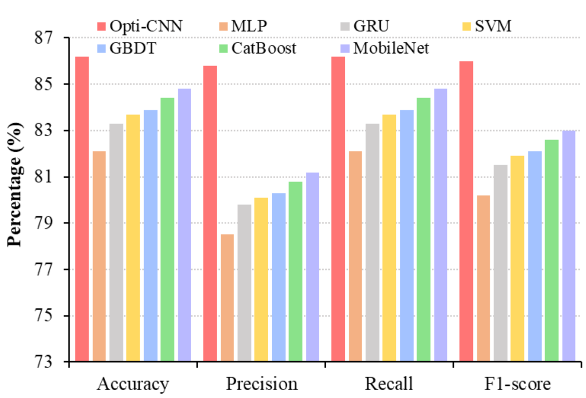

Figure 4. Comparison of performance of different models.

Model performance

The proposed model, Opti-CNN, was compared with other existing models. The results showed that the accuracy, precision, recall, and F1-score of Opti-CNN were 86.2%, 85.8%, 86.2%, and 86%, respectively. The proposed Opti-CNN had the best performance regarding various performance indicators compared to the other models (Figure 4). The ROC curves of different models demonstrated that the area under the ROC curve of proposed Opti-CNN model was 0.90 at the maximum. Compared with other algorithms, the proposed Opti-CNN model had better performance (Figure 5).

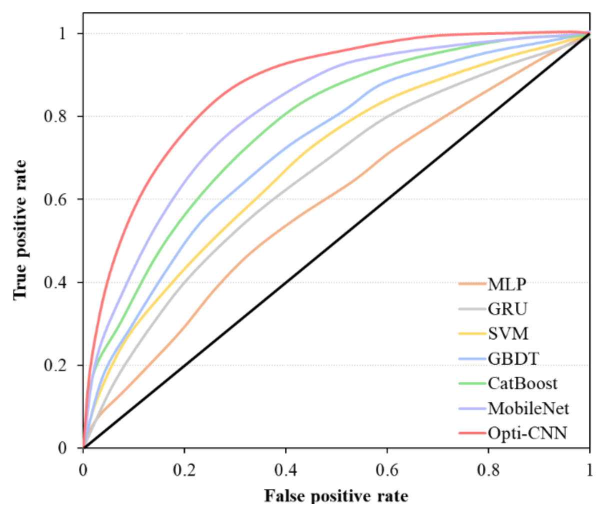

Figure 5. ROC curves of different models.

Model interpretability

This study focused on the prediction of health risks in elderly patients, comprehensively considering multiple factors and their respective weights across five dimensions including sociodemographic, disease, psychological, medication, and physiological. The feature importance analysis based on the LIME methodology indicated that the following factors exerted certain positive effects on health risks, which included age, multimorbidity (≥ 3 conditions), cardiovascular diseases, neurological diseases, endocrine and metabolic diseases, anxiety, depressive symptoms and fear of falling, polypharmacy (≥ 5 medications), use of antiepileptic and anticonvulsant drugs, frailty (frailty index ≥ 0.25), and nocturia (≥ 2 episodes/ night). Conversely, nutritional supplementation

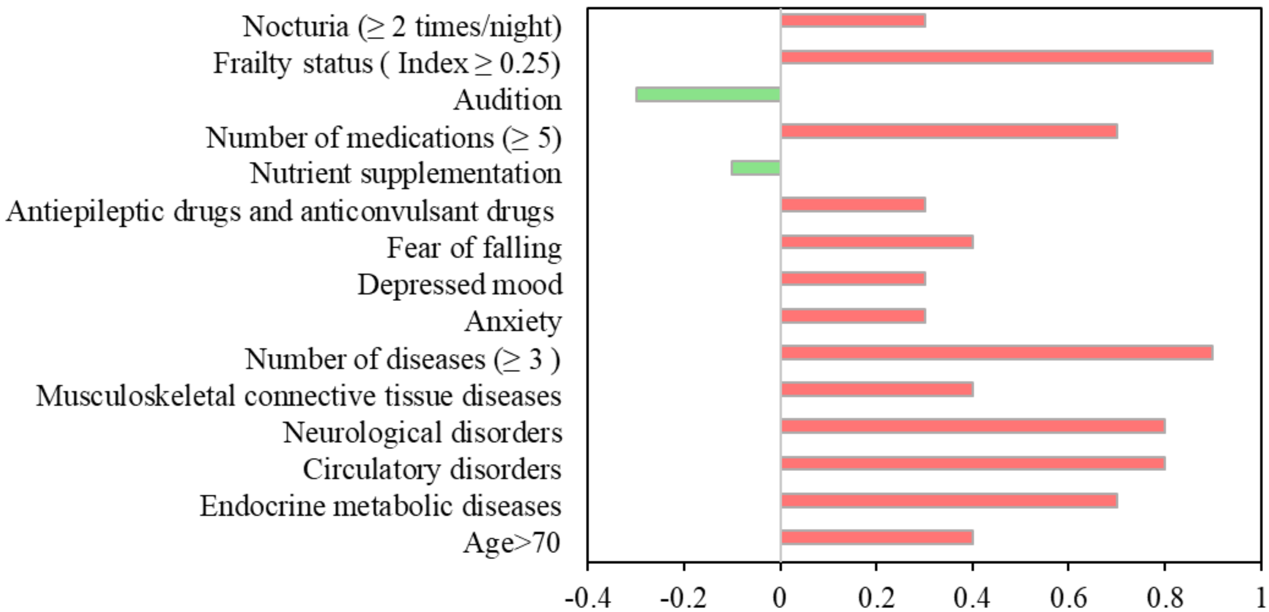

Figure 6. Feature variable weight chart based on the LIME method.

and hearing ability demonstrated certain negative effects on health risks (Figure 6). Through the analysis of SHAP, each risk factor's contribution to the health risk of elderly patients was clarified. The coexistence of multiple diseases (≥ 3 kinds) and weakness (weakness index ≥ 0.25) were the primary driving factors affecting the health risk of elderly patients, and the contribution degree of SHAP reached 0.9. The result emphasized the core position of nerve and motor function in fall risk assessment. Cognitive dysfunction (0.75), multiple drug use (≥ 5 kinds, 0.7), and cardiovascular disease (0.7) had similar contributions. Skeletal muscle diseases (0.65), antihypertensive drugs (0.62), sedative and hypnotic drugs (0.6), antiepileptic and anticonvulsant drugs (0.55), hypoglycemic drugs (0.58), endocrine and metabolic diseases (0.55), and other factors also had certain influences. Among psychological factors, fear of falling (0.35), depression (0.28), and anxiety (0.12) had positive effects on health risks. The contribution of age > 70 years and nocturia (≥ 2 times/night) were relatively low, which were 0.45 and 0.3, respectively. Among the protective factors, nutritional supplements (SHAP value -0.42) and hearing function (SHAP value -0.38) had negative effects on health risks (Figure 7). The results of information gain analysis showed that the maximum information gain of nervous system diseases was 0.8, and the information gains of coexistence of multiple diseases (≥ 3 kinds) and multiple drugs (≥ 5 kinds) were tied for second place, both of which were 0.7. The information gain of people over 70 years old was 0.7. The number of nocturia ≥ 2 times/night, the information gains of weakness (weakness index ≥ 0.25), and gait balance ability were 0.45, 0.4, and 0.4, respectively. The information gain of endocrine and metabolic diseases was 0.35, and the use of antiepileptic and anticonvulsant drugs was 0.20. Among the psychological factors, the information gain of falling fear was 0.25, depression was 0.20, and anxiety was 0.10. Among the protective factors, the information gain of nutritional supplements was 0.35, and the information gain of hearing function was 0.30. The information gains of sedative-hypnotic drugs, cognitive dysfunction, cardiovascular diseases, skeletal muscle diseases, antihypertensive drugs, and hypoglycemic drugs were low, which were 0.15, 0.1, 0.1, 0.1, 0.1, and 0.05, respectively (Figure 8).

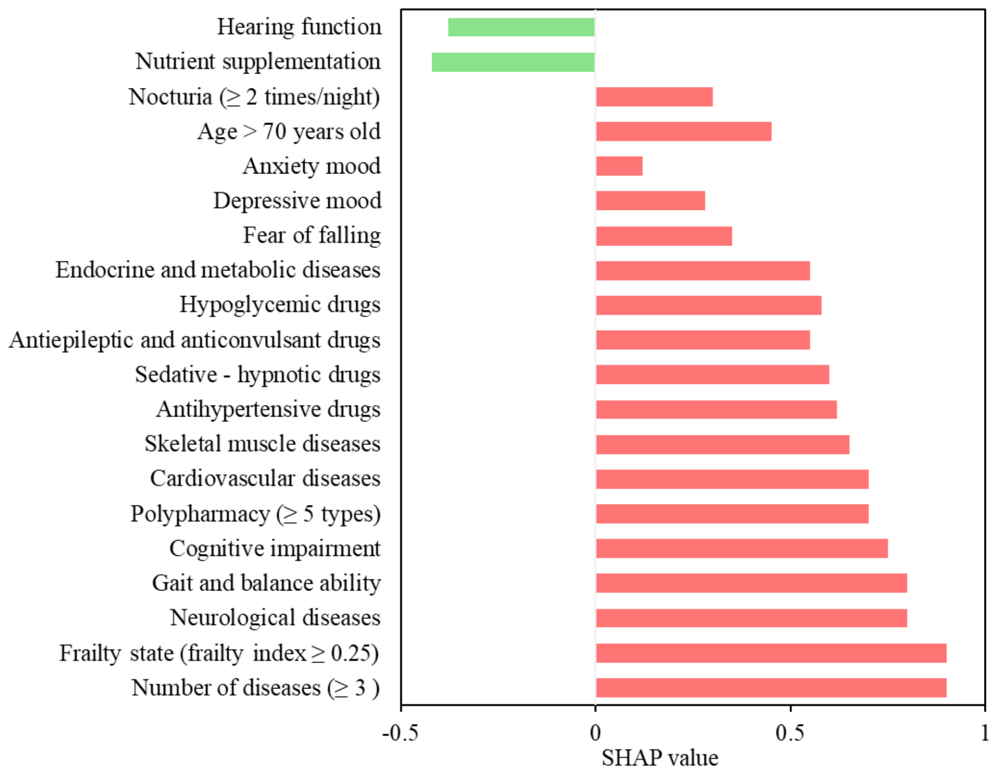

Figure 7. Feature importance ranking chart based on SHAP.

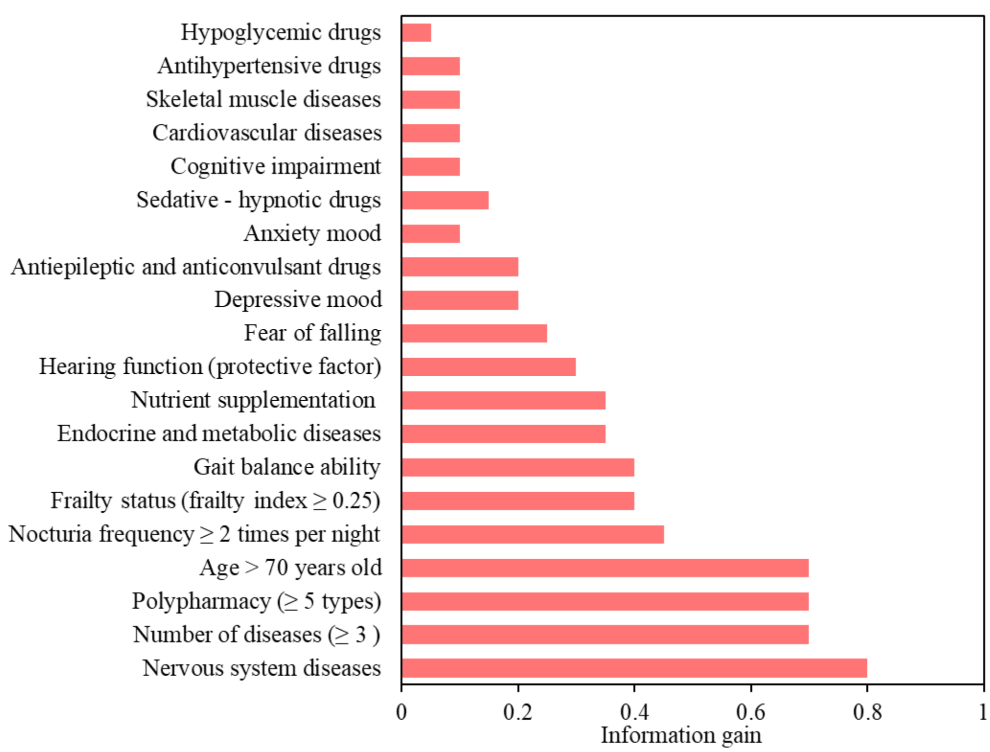

Figure 8. Feature importance ranking chart based on gain output.

Conclusion

This study collected clinical data from geriatric patients with multiple chronic conditions to construct an Opti-CNN health risk prediction model. The research incorporates both SHAP and LIME methodologies to interpret the model's predictions targeting in-hospital fall events. The proposed Opti-CNN model demonstrated superior performance regarding evaluation metrics to other algorithms. LIME, SHAP values, and information gain analyses collectively clarified the influence of various factors on health risks. The study developed a clinical decision support system that provided personalized recommendations. However, the research had several limitations, which included that the dataset might contain selection bias and incomplete information, the model's performance in predicting other adverse events required further validation, architectural optimization details needed more comprehensive description, interpretability methodologies warranted comparative integration and validation of result accuracy, and the practical utility of the decision support system necessitated clinical evaluation. Future work should include multi-center, large-sample validation and the development of dynamically updated models. This research provided an effective tool for health management in elderly populations and advanced the adoption of DL in healthcare.

References

1. Hemmeter UM, Ngamsri T. 2022. Körperliche Aktivität und psychische Gesundheit: Fokus Alter [Physical Activity and Mental Health in the Elderly]. Praxis (Bern 1994). 110(4):193-198.
2. Rimal Y, Sharma N, Paudel S, Alsadoon A, Koirala MP, Gill S. 2025. Comparative analysis of heart disease prediction using logistic regression, SVM, KNN, and random forest with cross-validation for improved accuracy. Sci Rep. 15(1):13444.
3. Volinsky-Fremond S, Horeweg N, Andani S, Barkey Wolf J, Lafarge MW, de Kroon CD, *et al*. 2024. Prediction of recurrence risk in endometrial cancer with multimodal deep learning. Nat Med. 30(7):1962-1973.
4. Guido R, Ferrisi S, Lofaro D, Conforti D. 2024. An overview on the advancements of support vector machine models in healthcare applications: A review. Information. 15(4):235.
5. Niu T, Cao S, Cheng J, Zhang Y, Zhang Z, Xue R, *et al*. 2024. An explainable predictive model for anxiety symptoms risk among Chinese older adults with abdominal obesity using a machine learning and SHapley Additive exPlanations approach. Front Psychiatry. 15:1451703.
6. Song Y, Zhang D, Wang Q, Liu Y, Chen K, Sun J, *et al*. 2024. Prediction models for postoperative delirium in elderly patients with machine-learning algorithms and SHapley Additive exPlanations. Transl Psychiatry. 14(1):57.
7. Lu SC, Brown RJ, Michalowski M. 2021. A clinical decision support system design framework for nursing practice. ACI Open. 5(02):e84-e93.
8. Jabbour G, Nolin-Lapalme A, Tastet O, Corbin D, Jordà P, Sowa A, *et al*. 2024. Prediction of incident atrial fibrillation using deep learning, clinical models, and polygenic scores. Eur Heart J. 45(46):4920-4934.
9. Qian X, Li Y, Zhang X, Guo H, He J, Wang X, *et al*. 2022. A cardiovascular disease prediction model based on routine physical examination indicators using machine learning methods: A cohort study. Front Cardiovasc Med. 9:854287.
10. Holmström IK, Gustafsson S, Wesström J, Skoglund K. 2019. Telephone nurses' use of a decision support system: An observational study. Nurs Health Sci. 21(4):501-507.
11. Hao Y, Usama M, Yang J, Hossain MS, Ghoneim A. 2019. Recurrent convolutional neural network based multimodal disease risk prediction. Future Gener Comput Syst. 92:76-83.
12. Li P, Hao H, Bai Y, Li Y, Mao X, Xu J, *et al*. 2022. Convolutional neural networks-based health risk modelling of some heavy metals in a soil-rice system. Sci Total Environ. 838:156466.
13. Selwal A, Raoof I. 2020. A multi-layer perceptron based intelligent thyroid disease prediction system. Indones J Electr Eng Comput Sci. 17(1):524-533.
14. Ali AA, Hassan HS, Anwar EM. 2020. Heart diseases diagnosis based on a novel convolution neural network and gate recurrent unit technique. IEEE. 2020:145-150.
15. Baydogan C. 2025. Lightweight deep learning architectures for ophthalmic disease detection: MobileNet variants applied to glaucoma classification. Electron Lett Sci Eng. 21(2):123-135.
16. Sharma A, Kaur S, Memon N, Fathima AJ, Ray S, Bhatt MW. 2021. Alzheimer's patients detection using support vector machine (SVM) with quantitative analysis. Neurosci Inform. 1(3):100012.
17. Kiran S, Reddy GR, Dorthi K. 2023. A gradient boosted decision tree with binary spotted hyena optimizer for cardiovascular disease detection and classification. Healthc Anal. 3:100173.
18. Al-Sarem M, Saeed F, Boulila W, Emara AH, Al-Mohaimeed M, Errais M. 2020. Feature selection and classification using CatBoost method for improving the performance of predicting Parkinson's disease. In: Advances on Smart and Soft Computing: Proceedings of ICACIn 2020. Singapore: Springer Singapore; 2020:189-199.